

This discussion paper is/has been under review for the journal The Cryosphere (TC).
Please refer to the corresponding final paper in TC if available.

Manufactured solutions and the numerical verification of isothermal, nonlinear, three-dimensional Stokes ice-sheet models

W. Leng¹, L. Ju^{2,3}, M. Gunzburger⁴, and S. Price⁵

¹State Key Laboratory of Scientific and Engineering Computing, Chinese Academy of Sciences, Beijing 100190, China

²Department of Mathematics, University of South Carolina, Columbia, SC 29208, USA

³Beijing Computational Science Research Center, Beijing 100084, China

⁴Department of Scientific Computing, Florida State University, Tallahassee, FL 32306, USA

⁵Theoretical Division, Los Alamos National Laboratory, Los Alamos, NM 87545, USA

Received: 9 June 2012 – Accepted: 22 June 2012 – Published: 20 July 2012

Correspondence to: L. Ju (ju@math.sc.edu), M. Gunzburger (gunzburg@fsu.edu)

Published by Copernicus Publications on behalf of the European Geosciences Union.

Abstract

The technique of manufactured solutions is used for verification of computational models in many fields. In this paper we construct manufactured solutions for models of three-dimensional, isothermal, nonlinear Stokes flow in glaciers and ice sheets. The solution construction procedure starts with kinematic boundary conditions and is mainly based on the solution of a first-order partial differential equation for the ice velocity that satisfies the incompressibility condition. The manufactured solutions depend on the geometry of the ice sheet and other model parameters. Initial conditions are taken from the periodic geometry of a standard problem of the ISMIP-HOM benchmark tests and altered through the manufactured solution procedure to generate an analytic solution for the time-dependent flow problem. We then use this manufactured solution to verify a parallel, high-order accurate, finite element Stokes ice-sheet model. Results from the computational model show excellent agreement with the manufactured analytic solutions.

1 Introduction

Model verification and validation are crucial steps in the development and testing of computational models. Verification is the process of determining if a particular implementation and solution of a given mathematical model (for example through some choice of model discretization and numerical solution algorithms) is complete and error free. Validation aims to answer the entirely separate question of whether or not a given mathematical model is an accurate representation of the real world process it aims to mimic. Manufactured analytical solutions provide one means for performing model verification.

The importance of ice-sheet modeling in climate studies is highlighted in, e.g. Alley et al. (2012) and the need for verified and validated models is discussed in Pachauri et al. (2007). The goal of this paper is to provide a means, through the use

TCD

6, 2689–2714, 2012

Manufactured solutions of 3-D Stokes ice-sheet models

W. Leng et al.

Title Page

Abstract

Introduction

Conclusions

References

Tables

Figures

⏪

⏩

◀

▶

Back

Close

Full Screen / Esc

Printer-friendly Version

Interactive Discussion



of manufactured solutions, for the verification of three-dimensional ice-sheet models as a necessary step for providing accurate, science-based predictions of ice-sheet changes over climatic time scales. Manufactured analytical solutions have been used previously by the ice-sheet modeling community (Bahr, 1996; Bueler et al., 2005, 2007; Sargent and Fastook, 2010).

The nonlinear, three-dimensional (3-D) Stokes model is generally accepted as the gold standard for the modeling of ice flow within glaciers and ice sheets (Le Meur et al., 2004; Gagliardini et al., 2008; Burstedde et al., 2009; Zhang et al., 2011; Larour et al., 2012; Leng et al., 2012). The more commonly used shallow-ice, shallow-shelf, L1L2, and first-order approximations are reduced forms of the 3-D Stokes model that are numerically simpler and computationally cheaper to solve, but with an attendant loss of fidelity in some situations (see discussions in Dukowicz et al., 2010; Schoof and Hindmarsh, 2010, and the references cited therein). As an example, the ISMIP-HOM project (Pattyn et al., 2008) compared diagnostic output from a number of “higher-order” (i.e. those accounting for horizontal stress gradients) and Stokes flow ice-sheet models on idealized domains. For certain combinations of domain aspect ratio, basal roughness, and basal sliding conditions, higher-order and Stokes model solutions differ significantly. Ideally, diagnostic output from Stokes models should first be compared with that from lower-order approximations in order to identify portions of the model domain for which the Stokes (relatively expensive) versus the reduced (relatively cheaper) sets of equations apply with sufficient accuracy (e.g. Morlighem et al., 2010). Such an approach would allow for an ideal tradeoff between model accuracy and expense (e.g. Seroussi et al., 2012).

Manufactured solutions for the verification of isothermal Stokes ice sheet models were recently proposed by Sargent and Fastook (2010) for two and three-dimensional model domains. In their approach, the major task in the construction of the analytic solution is to solve a first-order partial differential equation. However, due to essential errors in their solution method for this key part in the three-dimensional case, the Sargent and Fastook (2010) manufactured solutions (both the general form of the solution

Manufactured solutions of 3-D Stokes ice-sheet models

W. Leng et al.

Title Page

Abstract

Introduction

Conclusions

References

Tables

Figures

⏪

⏩

◀

▶

Back

Close

Full Screen / Esc

Printer-friendly Version

Interactive Discussion

Manufactured solutions of 3-D Stokes ice-sheet models

W. Leng et al.

Title Page

Abstract

Introduction

Conclusions

References

Tables

Figures

⏪

⏩

◀

▶

Back

Close

Full Screen / Esc

Printer-friendly Version

Interactive Discussion

and the solution for the specific geometry) for the 3-D Stokes model are incorrect. In Leng et al. (2012), the authors “extruded” the correct 2-D analytical solution of Sargent and Fastook (2010) to a third dimension and used it to verify the output from their Stokes ice-sheet model. This method of generating and applying a 3-D manufactured solution is far from optimal, as the 3-D model is applied in a 2-D mode, leaving parts of the 3-D model untested. In this paper, we rectify this deficiency by generating fully 3-D manufactured solutions for the validation of isothermal, nonlinear Stokes models of ice flow.

The paper is organized as follows. In Sect. 2, we present the 3-D nonlinear Stokes equations for modeling isothermal ice sheets along with some related boundary conditions. In Sect. 3, we derive in detail the manufactured analytical solutions for the 3-D, time-dependent Stokes ice-sheet model. In Sect. 4, we use the manufactured solutions for the numerical verification of the parallel finite element ice-sheet model of Leng et al. (2012). We finish in Sect. 5 with concluding remarks.

2 Governing equations of the Stokes ice-sheet model

2.1 Ice dynamics and evolution

The dynamical behavior of ice sheets is modeled by the Stokes equations for an incompressible, power-law viscous fluid in a low Reynolds-number flow. Letting $[0, t_{\max}]$ denote the time interval of interest and Ω_t the three-dimensional spatial domain occupied by the ice sheet, we have

Manufactured solutions of 3-D Stokes ice-sheet models

W. Leng et al.

Title Page

Abstract

Introduction

Conclusions

References

Tables

Figures

◀

▶

◀

▶

Back

Close

Full Screen / Esc

Printer-friendly Version

Interactive Discussion

$$\frac{\partial(2\mu\frac{\partial u}{\partial x} + p)}{\partial x} + \frac{\partial(\mu(\frac{\partial u}{\partial y} + \frac{\partial v}{\partial x}))}{\partial y} + \frac{\partial(\mu(\frac{\partial u}{\partial z} + \frac{\partial w}{\partial x}))}{\partial z} = 0, \quad (1)$$

$$\frac{\partial(\mu(\frac{\partial u}{\partial y} + \frac{\partial v}{\partial x}))}{\partial x} + \frac{\partial(2\mu\frac{\partial v}{\partial y} + p)}{\partial y} + \frac{\partial(\mu(\frac{\partial v}{\partial z} + \frac{\partial w}{\partial y}))}{\partial z} = 0, \quad (2)$$

$$\frac{\partial(\mu(\frac{\partial u}{\partial z} + \frac{\partial w}{\partial x}))}{\partial x} + \frac{\partial(\mu(\frac{\partial v}{\partial y} + \frac{\partial w}{\partial z}))}{\partial y} + \frac{\partial(2\mu\frac{\partial w}{\partial z} + p)}{\partial z} = \rho g, \quad (3)$$

$$\frac{\partial u}{\partial x} + \frac{\partial v}{\partial y} + \frac{\partial w}{\partial z} = 0, \quad (4)$$

where $(u, v, w)^T$ denotes the velocity, p the pressure, ρ the density of ice, and g the gravitational acceleration. The effective viscosity μ is defined by Glen's flow (Nye, 1957) law as

$$\mu = \frac{1}{2} A^{-\frac{1}{n}} \left[\frac{1}{4} \left(\frac{\partial u}{\partial y} + \frac{\partial v}{\partial x} \right)^2 + \frac{1}{4} \left(\frac{\partial u}{\partial z} + \frac{\partial w}{\partial x} \right)^2 + \frac{1}{4} \left(\frac{\partial v}{\partial z} + \frac{\partial w}{\partial y} \right)^2 - \frac{\partial u}{\partial x} \frac{\partial v}{\partial y} - \frac{\partial u}{\partial x} \frac{\partial w}{\partial z} - \frac{\partial v}{\partial y} \frac{\partial w}{\partial z} \right]^{\frac{1-n}{2n}} \quad (5)$$

with n the power-law exponent ($n = 3$ is generally assumed for modeling ice), and A the temperature-dependent deformation rate factor. In the isothermal case, A is taken as a spatially and temporally uniform constant.

If the top surface of the ice sheet is allowed to evolve in time, then a prognostic equation describing the evolution of that free surface is included. The ice-sheet domain Ω_t at a time t can be defined as

$$\Omega_t = \{(x, y, z) | b(x, y) \leq z \leq s(x, y, t) \text{ for } (x, y) \in \Omega_H, t \in [0, t_{\max}]\},$$

where Ω_H denotes the horizontal extent of the ice sheet, $s(x, y, t)$ defines the top surface elevation, and $b(x, y)$ defines the fixed bottom surface of the ice sheet. We denote the top surface as Γ_s and the bottom surface as Γ_b . The motion of the free surface is governed by the kinematic relation

$$5 \quad \frac{\partial s}{\partial t} + u \frac{\partial s}{\partial x} + v \frac{\partial s}{\partial y} - w = a, \quad (x, y) \in \Omega_H, \quad (6)$$

on the top surface of the ice sheet Γ_s , where a represents the surface mass balance (accumulation less ablation). Because the bed of the ice sheet is assumed to be fixed, we obtain a similar kinematic relation

$$u \frac{\partial b}{\partial x} + v \frac{\partial b}{\partial y} - w = 0, \quad (x, y) \in \Omega_H, \quad (7)$$

10 on the bottom surface Γ_b .

2.2 Boundary equations

At the top surface Γ_s of the ice sheet, we impose a stress free boundary condition

$$\frac{1}{r_s} \left[-\frac{\partial s}{\partial x} \left(2\mu \frac{\partial u}{\partial x} + \rho \right) - \frac{\partial s}{\partial y} \mu \left(\frac{\partial u}{\partial y} + \frac{\partial v}{\partial x} \right) + \mu \left(\frac{\partial u}{\partial z} + \frac{\partial w}{\partial x} \right) \right] = 0, \quad (8)$$

$$\frac{1}{r_s} \left[-\frac{\partial s}{\partial x} \mu \left(\frac{\partial u}{\partial y} + \frac{\partial v}{\partial x} \right) - \frac{\partial s}{\partial y} \left(2\mu \frac{\partial v}{\partial y} + \rho \right) + \mu \left(\frac{\partial v}{\partial z} + \frac{\partial w}{\partial y} \right) \right] = 0, \quad (9)$$

$$15 \quad \frac{1}{r_s} \left[-\frac{\partial s}{\partial x} \mu \left(\frac{\partial u}{\partial z} + \frac{\partial w}{\partial x} \right) - \frac{\partial s}{\partial y} \mu \left(\frac{\partial v}{\partial y} + \frac{\partial w}{\partial z} \right) + \left(2\mu \frac{\partial w}{\partial z} + \rho \right) \right] = 0, \quad (10)$$

where $r_s = \sqrt{1 + \left(\frac{\partial s}{\partial x}\right)^2 + \left(\frac{\partial s}{\partial y}\right)^2}$.

The bottom bedrock surface Γ_b of the ice sheet can be decomposed into two parts, $\Gamma_{b,fix}$ at which the ice sheet is fixed to the bottom bedrock and $\Gamma_{b,slid}$ at which it is allowed

Manufactured solutions of 3-D Stokes ice-sheet models

W. Leng et al.

Title Page

Abstract

Introduction

Conclusions

References

Tables

Figures

◀

▶

◀

▶

Back

Close

Full Screen / Esc

Printer-friendly Version

Interactive Discussion



to slip. We apply the zero velocity (no-slip and no-penetration) boundary condition

$$u = v = w = 0 \quad (11)$$

on the fixed part of the basal boundary $\Gamma_{b,fix}$ and the Rayleigh friction boundary condition

$$\frac{1}{r_b} \left[-\frac{\partial b}{\partial x} \left(2\mu \frac{\partial u}{\partial x} + \rho \right) - \frac{\partial b}{\partial y} \mu \left(\frac{\partial u}{\partial y} + \frac{\partial v}{\partial x} \right) + \mu \left(\frac{\partial u}{\partial z} + \frac{\partial w}{\partial x} \right) \right] = -\beta^2 u, \quad (12)$$

$$\frac{1}{r_b} \left[-\frac{\partial b}{\partial x} \mu \left(\frac{\partial u}{\partial y} + \frac{\partial v}{\partial x} \right) - \frac{\partial b}{\partial y} \left(2\mu \frac{\partial v}{\partial y} + \rho \right) + \mu \left(\frac{\partial v}{\partial z} + \frac{\partial w}{\partial y} \right) \right] = -\beta^2 v, \quad (13)$$

$$u \frac{\partial b}{\partial x} + v \frac{\partial b}{\partial y} - w = 0, \quad (14)$$

on the sliding part $\Gamma_{b,sld}$, where $r_b = \sqrt{1 + \left(\frac{\partial b}{\partial x}\right)^2 + \left(\frac{\partial b}{\partial y}\right)^2}$, and the parameter β^2 denotes a given, positive sliding coefficient.

Note that both the zero velocity boundary condition and the friction boundary condition automatically imply the kinematic Eq. (7) according to Eqs. (11) and (14). If $\Gamma_{b,fix} = \Gamma_b$, we have a pure zero velocity boundary condition on the bedrock surface; if $\Gamma_{b,sld} = \Gamma_b$, we have a pure sliding boundary condition; otherwise, we have a mixed boundary condition.

We also point out that, in general, $b(x, y) \neq s(x, y, t)$ along the boundary of Ω_H so that the ice sheet may also have a lateral boundary Γ_ℓ with some appropriate boundary conditions posed there; for example, a periodic boundary condition or a zero boundary condition could be applied there.

Manufactured solutions of 3-D Stokes ice-sheet models

W. Leng et al.

Title Page

Abstract

Introduction

Conclusions

References

Tables

Figures

⏪

⏩

◀

▶

Back

Close

Full Screen / Esc

Printer-friendly Version

Interactive Discussion



3 Manufactured Analytic Solutions

3.1 A general form of the analytic solution

Following the work of Sargent and Fastook (2010), we start from the kinematic boundary conditions (6) and (7) on the top and bottom surfaces, respectively and set the vertical velocity w by linearly interpolating u and v from the top to bottom bedrock surfaces as follows:

$$w(x, y, z, t) = u(x, y, z, t) \left(\frac{\partial b}{\partial x} \frac{s-z}{s-b} + \frac{\partial s}{\partial x} \frac{z-b}{s-b} \right) + v(x, y, z, t) \left(\frac{\partial b}{\partial y} \frac{s-z}{s-b} + \frac{\partial s}{\partial y} \frac{z-b}{s-b} \right) + \left(\frac{\partial s}{\partial t} - a \right) \frac{z-b}{s-b}. \quad (15)$$

Differentiating Eq. (15) with respect to z then gives

$$\frac{\partial w}{\partial z} = \frac{\partial u}{\partial z} \left(\frac{\partial b}{\partial x} \frac{s-z}{s-b} + \frac{\partial s}{\partial x} \frac{z-b}{s-b} \right) + u \frac{\frac{\partial s}{\partial x} - \frac{\partial b}{\partial x}}{s-b} + \frac{\partial v}{\partial z} \left(\frac{\partial b}{\partial y} \frac{s-z}{s-b} + \frac{\partial s}{\partial y} \frac{z-b}{s-b} \right) + v \frac{\frac{\partial s}{\partial y} - \frac{\partial b}{\partial y}}{s-b} + \frac{1}{s-b} \left(\frac{\partial s}{\partial t} - a \right). \quad (16)$$

Now substituting Eq. (16) into the incompressibility Eq. (4), we obtain a first-order quasi-linear partial differential equation with three independent variables x , y , z , and two dependent variables u , v :

$$\frac{\partial u}{\partial x} + \frac{\partial u}{\partial z} \left(\frac{\partial b}{\partial x} \frac{s-z}{s-b} + \frac{\partial s}{\partial x} \frac{z-b}{s-b} \right) + u \frac{\frac{\partial s}{\partial x} - \frac{\partial b}{\partial x}}{s-b} + \frac{\partial v}{\partial y} + \frac{\partial v}{\partial z} \left(\frac{\partial b}{\partial y} \frac{s-z}{s-b} + \frac{\partial s}{\partial y} \frac{z-b}{s-b} \right) + v \frac{\frac{\partial s}{\partial y} - \frac{\partial b}{\partial y}}{s-b} + \frac{1}{s-b} \left(\frac{\partial s}{\partial t} - a \right) = 0. \quad (17)$$

dependent variable v :

$$\frac{\partial v}{\partial y} + \frac{\partial v}{\partial z} \left(\frac{\partial b}{\partial y} \frac{s-z}{s-b} + \frac{\partial s}{\partial y} \frac{z-b}{s-b} \right) + v \frac{\frac{\partial h}{\partial y}}{h} + c_x(1 + \gamma_1) \frac{\partial h}{\partial x} h^{\gamma_1-1} (1 - d^{\lambda_1}) + \frac{1}{h} \left(\frac{\partial s}{\partial t} - a \right) = 0. \quad (25)$$

5 The characteristic equations of Eq. (25) can be found as

$$\frac{dy}{1} = \frac{dz}{\frac{\partial b}{\partial y} \frac{s-z}{s-b} + \frac{\partial s}{\partial y} \frac{z-b}{s-b}} = \frac{dv}{v \frac{\frac{\partial h}{\partial y}}{h} + c_x(1 + \gamma_1) \frac{\partial h}{\partial x} h^{\gamma_1-1} (1 - d^{\lambda_1}) + \frac{1}{h} \left(\frac{\partial s}{\partial t} - a \right)}. \quad (26)$$

Note that the first-order partial differential Eq. (25) does not need initial conditions. To solve it we first need to find two independent integrable identities that, when integrated, provide equations such as

$$10 \begin{cases} \phi(x, y, z, v) = c_1, \\ \psi(x, y, z, v) = c_2, \end{cases} \quad (27)$$

where c_1 and c_2 are two underdetermined constants. Then, the solution of Eq. (25) can be written as

$$\theta(\phi, \psi) = 0, \quad (28)$$

where θ is an arbitrary smooth function of ϕ and ψ .

15 The first integral can be deduced from

$$\frac{dy}{1} = \frac{dz}{\frac{\partial b}{\partial y} \frac{s-z}{s-b} + \frac{\partial s}{\partial y} \frac{z-b}{s-b}}, \quad (29)$$

Manufactured solutions of 3-D Stokes ice-sheet models

W. Leng et al.

Title Page

Abstract

Introduction

Conclusions

References

Tables

Figures

⏪

⏩

◀

▶

Back

Close

Full Screen / Esc

Printer-friendly Version

Interactive Discussion



from which we then have

$$d\left(\frac{z-b}{s-b}\right) = 0, \quad (30)$$

implying that

$$\frac{z-b}{s-b} = c_1. \quad (31)$$

5 The second integral can be deduced from

$$\frac{dy}{1} = \frac{dv}{\frac{\partial h}{\partial y} + c_x(1 + \gamma_1)\frac{\partial h}{\partial x}h^{\gamma_1-1}(1 - d^{\lambda_1}) + \frac{1}{h}\left(\frac{\partial s}{\partial t} - a\right)}, \quad (32)$$

from which we then have

$$d(hv) = -c_x(1 + \gamma_1) \left[1 - \left(\frac{s-z}{s-b}\right)^{\lambda_1} \right] \frac{\partial h}{\partial x} h^{\gamma_1} dy - \left(\frac{\partial s}{\partial t} - a\right) dy. \quad (33)$$

Note that $d\left(\frac{z-b}{s-b}\right) = 0$, in which case the integration of Eq. (33) gives

$$10 hv = -c_x(1 + \gamma_1) \left[1 - \left(\frac{s-z}{s-b}\right)^{\lambda_1} \right] \int \frac{\partial h}{\partial x} h^{\gamma_1} dy - \int \left(\frac{\partial s}{\partial t} - a\right) dy + c_2. \quad (34)$$

The combination of Eqs. (28), (31) and (34) implies that the general solution of the Eq. (25) can be written as

$$\begin{aligned} \theta \left(v(s-b) + c_x(1 + \gamma_1) \left[1 - \left(\frac{s-z}{s-b}\right)^{\lambda_1} \right] \int \left(\frac{\partial s}{\partial x} - \frac{\partial b}{\partial x}\right) (s-b)^{\gamma_1} dy \right. \\ \left. + \int \left(\frac{\partial s}{\partial t} - a\right) dy, \frac{z-b}{s-b} \right) = 0 \end{aligned} \quad (35)$$

15

for some smooth function $\theta(\cdot, \cdot)$.

To better represent the relationship between the velocity v and the depth d , we choose the function θ as

$$\theta(\phi, \psi) = \phi - c_y[1 - (1 - \psi)^{\lambda_2}] + c_{by},$$

- 5 where λ_2 , c_y and c_{by} are again some parameters. It is then easy to verify that v can be written in the following form

$$v(x, y, z, t) = \frac{c_y}{s-b} \left[1 - \left(\frac{s-z}{s-b} \right)^{\lambda_2} \right] + c_{by} \frac{1}{s-b} - \frac{c_x}{s-b} (1 + \gamma_1) \left[1 - \left(\frac{s-z}{s-b} \right)^{\lambda_1} \right] \\ \cdot \int \left(\frac{\partial s}{\partial x} - \frac{\partial b}{\partial x} \right) (s-b)^{\gamma_1} dy - \frac{1}{s-b} \int \left(\frac{\partial s}{\partial t} - a \right) dy. \quad (36)$$

- 10 By combining (15), (21) and (36), we finally obtain the velocity solution derived from the kinetic boundary condition and the mass conservation equation as follows:

$$u(x, y, z, t) = c_x (s-b)^{\gamma_1} \left[1 - \left(\frac{s-z}{s-b} \right)^{\lambda_1} \right] + c_{bx} \frac{1}{s-b}, \quad (37)$$

$$v(x, y, z, t) = \frac{c_y}{s-b} \left[1 - \left(\frac{s-z}{s-b} \right)^{\lambda_2} \right] + c_{by} \frac{1}{s-b} - \frac{c_x}{s-b} (1 + \gamma_1) \left[1 - \left(\frac{s-z}{s-b} \right)^{\lambda_1} \right] \\ \cdot \int \left(\frac{\partial s}{\partial x} - \frac{\partial b}{\partial x} \right) (s-b)^{\gamma_1} dy - \frac{1}{s-b} \int \left(\frac{\partial s}{\partial t} - a \right) dy, \quad (38)$$

- 15 $w(x, y, z, t) = u(x, y, z, t) \left(\frac{\partial b}{\partial x} \frac{s-z}{s-b} + \frac{\partial s}{\partial x} \frac{z-b}{s-b} \right) + v(x, y, z, t) \left(\frac{\partial b}{\partial y} \frac{s-z}{s-b} + \frac{\partial s}{\partial y} \frac{z-b}{s-b} \right) \\ + \left(\frac{\partial s}{\partial t} - a \right) \frac{z-b}{s-b}. \quad (39)$

Manufactured solutions of 3-D Stokes ice-sheet models

W. Leng et al.

Title Page

Abstract

Introduction

Conclusions

References

Tables

Figures

◀

▶

◀

▶

Back

Close

Full Screen / Esc

Printer-friendly Version

Interactive Discussion

We choose the pressure solution to be that from the first-order ice-sheet model (Pat-
tyn, 2003):

$$p(x, y, z, t) = 2\mu \frac{\partial u}{\partial x} + 2\mu \frac{\partial v}{\partial y} - \rho g(s - z). \quad (40)$$

Equation (40) is derived from the Stokes momentum Eqs. (1)–(3) and the stress-
free boundary conditions (8)–(10) on the top surface through a first-order approxima-
tion. Consequently, the above manufactured analytic velocity and pressure solutions
Eqs. (37)–(40) do not satisfy exactly the momentum equations and the top surface
boundary equations. In order to maintain the equalities of these equations, some ad-
ditional compensation terms need be added to the right-hand sides of the Eqs. (1)–
(3) and Eqs. (8)–(10); these terms can be easily obtained by way of substituting the
above constructed analytical solution Eqs. (37)–(39) and (40) into the left-hand sides
of Eqs. (1)–(3) and (8)–(10). The explicit formulas for these compensation terms can be
calculated by using symbolic operations of the software “MAPLE” (we do not provide
them here because of their great length). We specially note that these extra terms are
of order $o(\delta)$ where δ denotes the aspect ration of the ice sheet so that a slightly mod-
ified Stokes model is obtained. Furthermore, if a sliding boundary condition is imposed
on the (full or partial) bottom bedrock surface, then the right-hand sides of Eqs. (12)
and (13) also need be slightly revised as in the above process.

3.2 A manufactured solution under a specific geometry for time-dependent ice flow

Given the surface and bed elevation (i.e. the geometry of an ice sheet), a specific
manufactured solution can be produced using the above procedure from Eqs. (37)–
(40). To simplify the formulation, we introduce some scaling parameters as follows: L
is the horizontal length scale (span) of the ice sheet, $Z = 1$ km is the vertical length
scale, $\delta = L/Z$ is the aspect ratio, $U = A L(2\rho gZ)^n$ is the horizontal velocity scale,
 $W = UZ/L$ is the vertical velocity scale, and $T = Z/W$ is the time scale. Note that we

Manufactured solutions of 3-D Stokes ice-sheet models

W. Leng et al.

Title Page

Abstract

Introduction

Conclusions

References

Tables

Figures

⏪

⏩

◀

▶

Back

Close

Full Screen / Esc

Printer-friendly Version

Interactive Discussion



and thus

$$-\frac{1}{s-b} \int_{\frac{L}{4}}^y \left(\frac{\partial s}{\partial t} - a \right) dy = 0. \quad (47)$$

Based on the above known functions s , b , a and the parameters γ_1 , λ_1 , λ_2 , c_x , c_y , c_{bx} , c_{by} and c_t , we construct the velocity solution (u, v, w) and the pressure solution p using Eqs. (37)–(40) for the time-dependent isothermal 3-D Stokes ice-sheet flow model. Note that this manufactured solution is obviously doubly periodic in velocity so that a periodic boundary condition on the lateral boundary Γ_1 ($\Gamma_1 \neq \emptyset$) is satisfied.

To further simplify the computation of the integral in Eq. (38), we specify $\gamma_1 = 0$ and $\lambda_1 = 4$, in which case that integral becomes

$$\begin{aligned} \frac{c_x}{s-b} (1+\gamma_1) \left[1 - \left(\frac{s-z}{s-b} \right)^{\lambda_1} \right] \int_{\frac{L}{4}}^y \left(\frac{\partial s}{\partial x} - \frac{\partial b}{\partial x} \right) (s-b)^{\gamma_1} dy \\ = \frac{1}{2} \frac{c_x}{s-b} \left[1 - \left(\frac{s-z}{s-b} \right)^4 \right] Z \cos \left(\frac{2\pi x}{L} \right) \cos \left(\frac{2\pi y}{L} \right) e^{-c_t t}. \end{aligned} \quad (48)$$

By using Eqs. (47) and (48), the velocity v defined in Eq. (38) can then be written as

$$\begin{aligned} v(x, y, z, t) = \frac{c_y}{s-b} \left[1 - \left(\frac{s-z}{s-b} \right)^{\lambda_2} \right] + c_{by} \frac{1}{s-b} \\ - \frac{1}{2} \frac{c_x}{s-b} \left[1 - \left(\frac{s-z}{s-b} \right)^4 \right] Z \cos \left(\frac{2\pi x}{L} \right) \cos \left(\frac{2\pi y}{L} \right) e^{-c_t t} \end{aligned} \quad (49)$$

which is much easier to calculate.

Manufactured solutions of 3-D Stokes ice-sheet models

W. Leng et al.

Title Page

Abstract

Introduction

Conclusions

References

Tables

Figures

◀

▶

◀

▶

Back

Close

Full Screen / Esc

Printer-friendly Version

Interactive Discussion



Additionally, we also let $c_{bx} = c_{by} = 0$; then, the velocity solution Eqs. (37)–(39) can be finally simplified as

$$u(x, y, z, t) = c_x \left(\frac{s-z}{s-b} \right)^4, \quad (50)$$

$$v(x, y, z, t) = \frac{c_y}{s-b} \left[1 - \left(\frac{s-z}{s-b} \right)^{\lambda_2} \right] - \frac{1}{2} \frac{c_x}{s-b} \left[1 - \left(\frac{s-z}{s-b} \right)^4 \right] Z \cos \left(\frac{2\pi x}{L} \right) \cos \left(\frac{2\pi y}{L} \right) e^{-c_1 t}, \quad (51)$$

$$w(x, y, z, t) = u(x, y, z, t) \left(\frac{\partial b}{\partial x} \frac{s-z}{s-b} + \frac{\partial s}{\partial x} \frac{z-b}{s-b} \right) + v(x, y, z, t) \left(\frac{\partial b}{\partial y} \frac{s-z}{s-b} + \frac{\partial s}{\partial y} \frac{z-b}{s-b} \right). \quad (52)$$

The solution (u, v, w) defined by Eqs. (50)–(52) satisfies a pure zero-velocity boundary condition on the whole bedrock surface $\Gamma_{b, \text{fix}} = \Gamma_b$.

Note that the velocity solution (u, v, w) of the (slightly modified) Stokes equation at the initial time $t = 0$ could easily be generated by setting the function $\xi(t) = 0$ in the exact time-dependent solutions. Similarly, the final geometrically stable ice-sheet configuration (i.e. a steady state with $\frac{ds}{dt} = 0$) will have a top surface with the elevation function given by $s_0(x, y) + \eta(x, y)$, generated by setting the function $\xi(t) = 1$ in the exact time-dependent solution.

4 Numerical verification of the Stokes ice sheet model of Leng et al. (2012)

We use the above manufactured analytic solutions to verify the parallel, high-order accurate, finite element, nonlinear Stokes ice sheet model in Leng et al. (2012). The model uses tetrahedral elements that are produced by first extruding a 2-D, triangular

in 424,364 DOFs. We divided the period $[0, 1000]$ uniformly with a time step $\Delta t = 1$ year to obtain a set of time steps $\{t_k\}_{k=0}^{1000}$. At each time step t_k , with $0 \leq k < 1000$, we compute the ice velocity from the numerical model and update the ice thickness at time t_{k+1} according to the free surface Eq. (6), using an explicit finite element discretization scheme (Leng et al., 2012).

Figure 2 shows the simulated changes of the ice-sheet geometry (the top and bottom surfaces) over time. Initially, the top surface is flat with a uniform slope (Fig. 1-left). When the final steady state is reached (at 1000 yr), the surface takes on the sinusoidal shape of the bed topography and the ice thickness is everywhere uniform and equal (Fig. 1-right). Figure 2 illustrates the evolution of the ice surface at 100 yr time intervals along a selected profile line. Note that all of the modeled ice surfaces agree very well with the exact solution $s(x, y, t)$.

Figure 3 presents the three velocity components and the pressure at the top surface of the ice at time $t = 0, 100$ and 1000 yr. Figure 4 shows the L^2 norm of the velocity and the pressure along the cross section at $y = L/4$ at the same times. Because the thickness is not uniform at the beginning of the simulation, the velocity and free surface co-evolve over the length of the simulation in order to increase or decrease the surface elevation, eventually leading to a uniform ice thickness everywhere in the domain. At the new steady state, ice flow is almost uniform horizontally but layered in the vertical.

5 Conclusions

In this paper, we derived manufactured solutions for isothermal, 3-D, nonlinear Stokes flow ice-sheet models. Their applicability for verifying numerical models was demonstrated through comparison to output from the finite element flow model of Leng et al. (2012). The solutions derived and demonstrated here should be of general use by the ice-sheet modeling community for the verification of nonlinear Stokes flow glacier and ice-sheet models.

Manufactured solutions of 3-D Stokes ice-sheet models

W. Leng et al.

Title Page

Abstract

Introduction

Conclusions

References

Tables

Figures



Back

Close

Full Screen / Esc

Printer-friendly Version

Interactive Discussion

Supplementary material related to this article is available online at:
<http://www.the-cryosphere-discuss.net/6/2689/2012/tcd-6-2689-2012-supplement.zip>.

Acknowledgements. Support for this work was provided through the Scientific Discovery through Advanced Computing (SciDAC) project funded by the US Department of Energy, Office of Science, Advanced Scientific Computing Research and Biological and Environmental Research, and also through the US National Science Foundation under grant number DMS-0913491.

References

- Alley, R. B. and Joughin, I.: Modeling ice-sheet flow, *Science*, 336, 551–552, 2012. 2690
- Bahr, D. B.: Analytical modeling of glacier dynamics, *Math. Geology*, 28, 229–251, doi:10.1007/BF02084214, 1996. 2691
- Bueler, E., Lingle, C. S., Kallen-Brown, J. A., Covey, D. N., and Bowman, L. N.: Exact solutions and verification of numerical models for isothermal ice sheets, *J. Glaciol.*, 51, 291–306, 2005. 2691
- Bueler, E., Brown, J., and Lingle, C. S.: Exact solutions to the thermomechanically coupled shallow-ice approximation: effective tools for verification, *J. Glaciol.*, 53, 499–516, 2007. 2691
- Burstedde, C., Ghattas, O., Stadler, G., Tu, T., and Wilcox, L. C.: Parallel scalable adjoint-based adaptive solution of variable-viscosity Stokes flow problems, *Comput. Methods Appl. Mech. Engrg.*, 198, 1691–1700, 2009. 2691
- Dukowicz, J. K., Price, S., and Lipscomb, W.: Consistent approximations and boundary conditions for ice-sheet dynamics from a principle of least action, *J. Glaciol.*, 56, 480–496, 2010. 2691
- Gagliardini, O. and Zwinger, T.: The ISMIP-HOM benchmark experiments performed using the Finite-Element code Elmer, *The Cryosphere*, 2, 67–76, doi:10.5194/tc-2-67-2008, 2008. 2691

Manufactured solutions of 3-D Stokes ice-sheet models

W. Leng et al.

Title Page

Abstract

Introduction

Conclusions

References

Tables

Figures

⏪

⏩

◀

▶

Back

Close

Full Screen / Esc

Printer-friendly Version

Interactive Discussion



Manufactured solutions of 3-D Stokes ice-sheet models

W. Leng et al.

Title Page

Abstract

Introduction

Conclusions

References

Tables

Figures

◀

▶

◀

▶

Back

Close

Full Screen / Esc

Printer-friendly Version

Interactive Discussion



- Larour, E., Seroussi, H., Morlighem, M., and Rignot, E.: Continental scale, high order, high spatial resolution, ice sheet modeling using the Ice Sheet System Model (ISSM), *J. Geophys. Res.*, 117, F01022, doi:10.1029/2011JF002140, 2012. 2691
- Le Meur, E., Gagliardini, O., Zwinger, T., and Ruokolainen, J.: Glacier flow modelling: a comparison of the shallow ice approximation and the full-Stokes solution, *C. R. Phys.*, 5, 709–722, 2004. 2691
- Leng, W., Ju, L., Gunzburger, M., Price, S., and Ringler, T.: A parallel high-order accurate finite element Stokes ice sheet model, *J. Geophys. Res.*, 117, F01001, doi:10.1029/2011JF001962, 2012. 2691, 2692, 2704, 2706
- Morlighem, M., Rignot, E., Seroussi, H., Larour, E., Dhia, H. B., and Aubry, D.: Spatial patterns of basal drag inferred using control methods for a full-Stokes and simpler models for Pine Island Glacier, West Antarctica, *J. Geophys. Res.*, 37, L14502, doi:10.1029/2010GL043853, 2010. 2691
- Nye, J.: The distribution of stress and velocity in glaciers and ice sheets, *Proc. R. Soc. London, Ser. A*, 239, 113–133, 1957. 2693
- Pachauri, R. K. and Reisinger, A. (eds.): Contribution of Working Groups I, II and III to the Fourth Assessment Report of the Intergovernmental Panel on Climate Change, IPCC, Geneva, Switzerland, 2007. 2690
- Pattyn, F.: A new 3-D higher-order thermomechanical ice-sheet model: basic sensitivity, ice-stream development and ice flow across subglacial lakes, *J. Geophys. Res.*, 108, 2382, doi:10.1029/2002JB002329, 2003. 2701
- Pattyn, F., Perichon, L., Aschwanden, A., Breuer, B., de Smedt, B., Gagliardini, O., Gudmundsson, G. H., Hindmarsh, R. C. A., Hubbard, A., Johnson, J. V., Kleiner, T., Kononov, Y., Martin, C., Payne, A. J., Pollard, D., Price, S., Rückamp, M., Saito, F., Souček, O., Sugiyama, S., and Zwinger, T.: Benchmark experiments for higher-order and full-Stokes ice sheet models (ISMIP-HOM), *The Cryosphere*, 2, 95–108, doi:10.5194/tc-2-95-2008, 2008. 2691, 2702
- Sargent, A. and Fastook, J. L.: Manufactured analytical solutions for isothermal full-Stokes ice sheet models, *The Cryosphere*, 4, 285–311, doi:10.5194/tc-4-285-2010, 2010. 2691, 2692, 2696, 2697
- Schoof, C. and Hindmarsh, R. C. A.: Thin-film flows with wall slip: an asymptotic analysis of higher order glacier flow models, *Q. J. Mech. Appl. Math.*, 63, 73–114, 2010. 2691

- Seroussi, H., Dhia, H. B., Morlighem, M., Larour, E., Rignot, E., and Aubry, D.: Coupling ice flow models of varying orders of complexity with the tiling method. *J. Glaciol.*, 58, 77600786, doi:10.3189/2012JoG11J195, 2012. 2691
- Zhang, H., Ju, L., Gunzburger, M., Ringler, T., and Price, S.: Coupled models and parallel simulations for three dimensional full-Stokes ice sheet modeling, *Numer. Math. Theo. Meth. Appl.*, 4, 359–381, 2011. 2691

Manufactured solutions of 3-D Stokes ice-sheet models

W. Leng et al.

Title Page

Abstract

Introduction

Conclusions

References

Tables

Figures

◀

▶

◀

▶

Back

Close

Full Screen / Esc

Printer-friendly Version

Interactive Discussion



Manufactured solutions of 3-D Stokes ice-sheet models

W. Leng et al.

Table 1. L^2 Errors in the velocity and pressure simulated by the parallel high-order accurate finite element Stokes ice sheet model at the initial state $t = 0$.

| Mesh | DOF | Velo. Error | Conv. Rate | Pres. Error | Conv. Rate |
|----------------------------|------------|-----------------------|------------|-----------------------|------------|
| $20 \times 20 \times 5$ | 56 184 | 2.67×10^1 | – | 1.91×10^1 | – |
| $40 \times 40 \times 10$ | 424 364 | 4.00×10^0 | 2.74 | 6.70×10^0 | 1.51 |
| $80 \times 80 \times 20$ | 3 296 724 | 3.16×10^{-1} | 3.66 | 1.82×10^{-1} | 1.88 |
| $160 \times 160 \times 40$ | 25 985 444 | 6.30×10^{-2} | 2.33 | 5.66×10^{-2} | 1.68 |

[Title Page](#)
[Abstract](#)
[Introduction](#)
[Conclusions](#)
[References](#)
[Tables](#)
[Figures](#)
[⏪](#)
[⏩](#)
[◀](#)
[▶](#)
[Back](#)
[Close](#)
[Full Screen / Esc](#)
[Printer-friendly Version](#)
[Interactive Discussion](#)

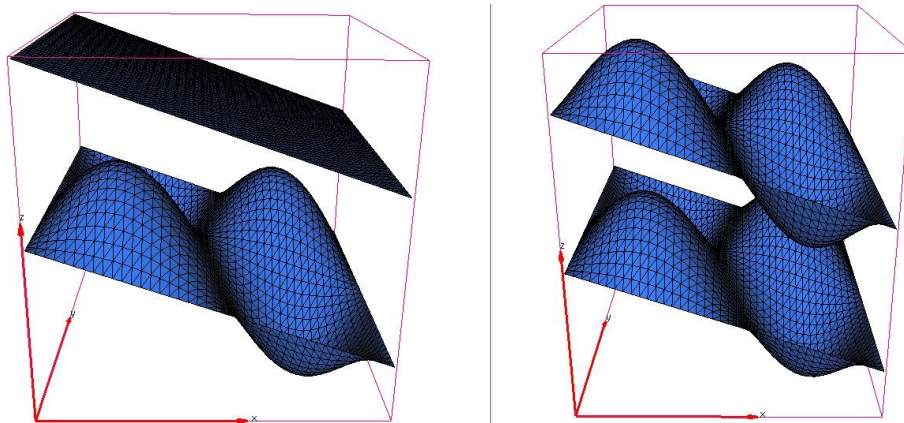



Fig. 1. Simulation results for the ice sheet geometry (the top and bottom surfaces) at the time $t = 0$ (left) and at the time $t = 1000$ yr (right).

Manufactured solutions of 3-D Stokes ice-sheet models

W. Leng et al.

| | |
|--------------------------|--------------|
| Title Page | |
| Abstract | Introduction |
| Conclusions | References |
| Tables | Figures |
| ⏪ | ⏩ |
| ◀ | ▶ |
| Back | Close |
| Full Screen / Esc | |
| Printer-friendly Version | |
| Interactive Discussion | |



Manufactured solutions of 3-D Stokes ice-sheet models

W. Leng et al.

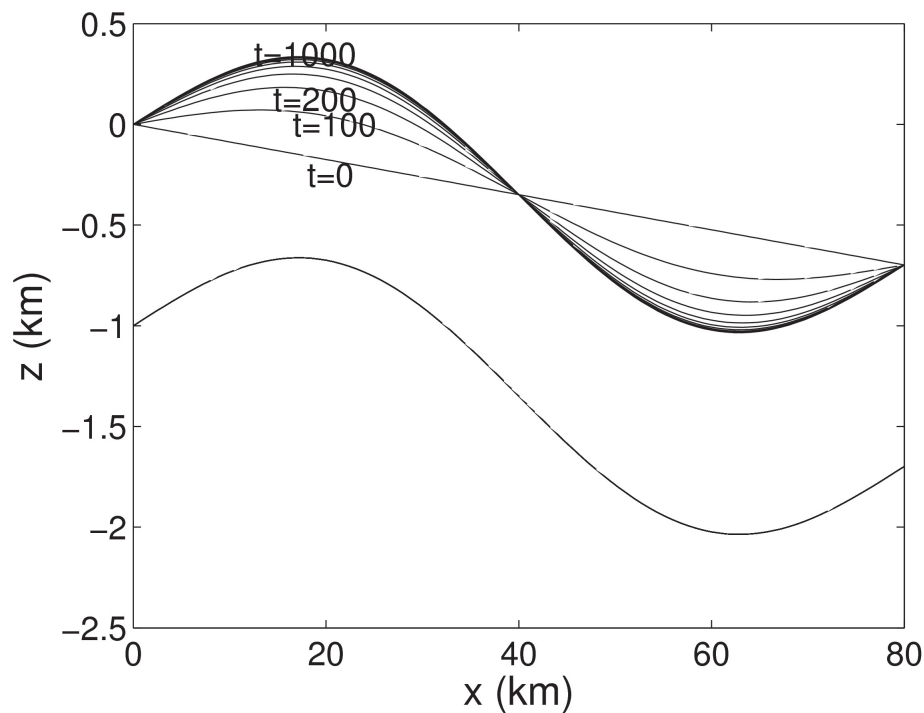


Fig. 2. x -direction profiles (km) of the ice sheet top and bottom surfaces at 100 yr time intervals from $t = 0$ to 1000 yr. Profiles are taken at $y = L/4$.

[Title Page](#)[Abstract](#)[Introduction](#)[Conclusions](#)[References](#)[Tables](#)[Figures](#)[◀](#)[▶](#)[◀](#)[▶](#)[Back](#)[Close](#)[Full Screen / Esc](#)[Printer-friendly Version](#)[Interactive Discussion](#)

Manufactured solutions of 3-D Stokes ice-sheet models

W. Leng et al.

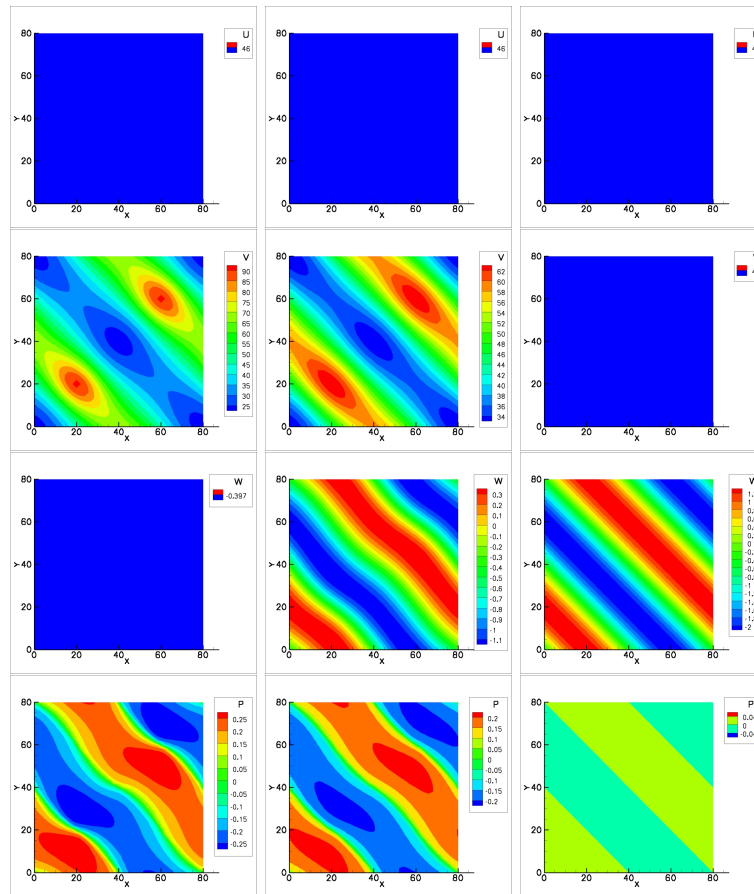


Fig. 3. Simulation results at the top surface of the ice sheet. From left to right: $t = 0, 100,$ and 1000 yr. From top to bottom: the velocity components u, v and w (m a^{-1}) and the pressure p .

Title Page

Abstract

Introduction

Conclusions

References

Tables

Figures

◀

▶

◀

▶

Back

Close

Full Screen / Esc

Printer-friendly Version

Interactive Discussion

Manufactured solutions of 3-D Stokes ice-sheet models

W. Leng et al.

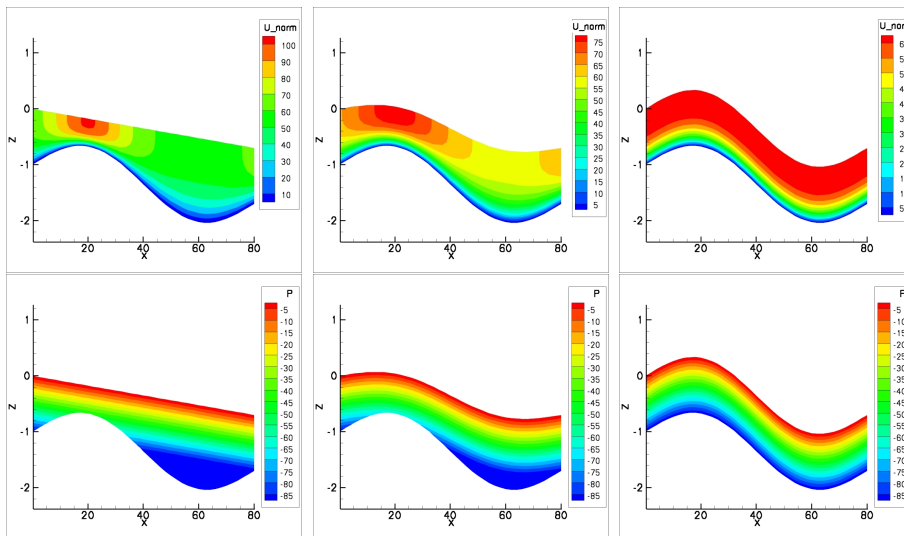


Fig. 4. Simulation results along the cross section $y = L/4$. From left to right: $t = 0, 100$ and 1000 yr. From top to bottom: the L^2 norm of the velocity (ma^{-1}) and the pressure p .

Discussion Paper | Discussion Paper | Discussion Paper | Discussion Paper | Discussion Paper

Title Page

Abstract Introduction

Conclusions References

Tables Figures

◀ ▶

◀ ▶

Back Close

Full Screen / Esc

Printer-friendly Version

Interactive Discussion

